balt5/zhl-hp/zhl-hp/zhl00409/zhl5181-09z | xppws | S=1 | 2/2/09 | 12:12 | Art: 191045 | Input-8000

Paper

MODELING THE ACUTE HEALTH EFFECTS OF ASTRONAUTS FROM EXPOSURE TO LARGE SOLAR PARTICLE EVENTS

Shaowen Hu,* Myung-Hee Y. Kim,* Gene E. McClellan,† and Francis A. Cucinotta‡

Fn1 *Abstract*—**Radiation exposure from Solar Particle Events (SPE) presents a significant health concern for astronauts for exploration missions outside the protection of the Earth's magnetic field, which could impair their performance and result in the possibility of failure of the mission. Assessing the potential for early radiation effects under such adverse conditions is of prime importance. Here we apply a biologically based mathematical model that describes the dose- and time-dependent early human responses that constitute the prodromal syndromes to consider acute risks from SPEs. We examine the possible early effects on crews from exposure to some historically large solar events on lunar and/or Mars missions. The doses and dose rates of specific organs were calculated using the Baryon radiation transport (BRYNTRN) code and a computerized anatomical man model, while the hazard of the early radiation effects and performance reduction were calculated using the Radiation-Induced Performance Decrement (RIPD) code. Based on model assumptions we show that exposure to these historical events would cause moderate early health effects to crew members inside a typical spacecraft or during extra-vehicular activities, if effective shielding and medical countermeasure tactics were not provided. We also calculate possible event worse cases (double intensity, multiple occurrences in a short period of time, etc.) to estimate the severity, onset and duration of various types of early illness. Uncertainties in the calculation due to limited data on relative biological effectiveness and dose-rate modifying factors for protons and secondary radiation, and the identification of sensitive sites in critical organs are discussed.**

Health Phys. 96(4):000–000; 2009

Key words: analysis, risk; computer calculations; health effects; radiation risk

INTRODUCTION

Solar Particle Events (SPE) occur quite often over the approximately 11-y solar cycle, but are highly episodic and almost unpredictable. They represent a major threat to crews of space exploration missions. During such events, the flux of protons with energy greater than 10 MeV may increase over background by 4 to 5 orders of magnitude for a period of several hours to a few days (Shea and Smart 1992). The hazards of exposure to these large doses have to be evaluated in the context of the high competing risks of vehicle or life support system failures. In addition to the risk of cancer (Cucinotta and Durante 2006; NCRP 2006) and other late effects such as the neuronal and heart disease risks (NCRP, 2006) and cataracts (Cucinotta et al. 2001), the appraisal of Acute Radiation Sickness (ARS) assumes prime importance because it can impair the performance capabilities of crew members and thereby threaten mission success.

ARS is a group of clinical syndromes developing acutely (within several seconds to 3 d) after high-dose, whole-body or significant partial-body ionizing radiation (Anno et al. 1989; Guskova et al. 2001). The manifestation of these syndromes reflects the disturbance of physiological processes of various cellular groups damaged by radiation. Hematopoietic cells, skin, epithelium, intestine, and vascular endothelium are among the most sensitive tissues of human body to ionizing radiation. Most ARS syndromes are directly related to these tissues, as well as the coupled regulation and adaptation systems (nervous, endocrine, cardiovascular systems) (Guskova et al. 2001 and references therein). It is generally agreed that there are three phases in the development of ARS: the prodromal phase, the latent phase, and the manifest phase. The severity and duration of each of these phases are dependent on the dose and dose rate. The prodromal phase refers to the first 48 h after exposure, but may persist up to 6 d (Alexander et al. 2007). The syndromes are dose-dependent and include hematopoietic depression, gastrointestinal distress (nausea, vomiting, and/or

* Division of Space Life Sciences, Universities Space Research Association, Houston, TX 77058; † Applied Research Associates, Inc., Arlington, VA 22203; ‡ NASA Johnson Space Center, Houston, TX 77058.

For the correspondence contact: Francis A. Cucinotta, NASA Johnson Space Center, 2101 NASA Parkway, Houston, TX 77058, or email at Francis.A.Cuciniotta@NASA.gov; or Shaowen Hu, Division of Space Life Sciences, Universities Space Research Association, Houston, TX 77058, or email at Shaowen.Hu-1@nasa.gov.

(*Manuscript accepted* 10 *October* 2008)
0017-9078/09/0

balt5/zhl-hp/zhl-hp/zhl00409/zhl5181-09z | xppws | S=1 | 2/2/09 | 12:12 | Art: 191045 | Input-8000

diarrhea), and neurological symptoms (including fatigability, weakness, headache, impaired cognition, disorientation, ataxia, seizures, and hypotension). The latent phase lasts about 2 to 20 d with a seeming improvement of most syndromes (except cytopenia), with duration correlating inversely with the absorbed dose. The manifest phase lasts from 2 to 60 d, with signs and symptoms expressed by various organs, and profound immune suppression predisposing the body to infection and sepsis. This phase is critical for radiation injury. Most patients surviving this phase will recover but are still at risk for intermediate effects such as pneumonitis and late effects (NCRP 2006; Guskova et al. 2001).

Calculations based on actual solar particle observations indicate that some large historical SPEs may induce moderate ARS in astronauts beyond low earth orbit (LEO) (Townsend et al. 1992; Wilson et al. 1990, 1991, 1997b, 1997c; Cucinotta et al. 1994b). To evaluate the possibility of ARS in space radiation environments, one should be aware of the difference between space radiation and common terrestrial radiation. While most ARS cases in the literature are caused by high-dose gamma rays and/or fission spectrum neutrons, large SPEs have an elemental composition that is dominated by protons with a small heavy-ion component (Mazur et al. 1992; Reames 1992). Thus, the relative biological effectiveness (RBE) of the different radiation components for causing the various endpoints of ARS must be understood to characterize the relevant responses in space (Cucinotta 1999; NCRP 2006). The energy spectra of SPEs varies from one event to the next, and therefore the dose distribution in tissue for solar protons will be quite distinct from gamma rays, showing more variability between tissues than gamma rays for most SPEs. In addition, many ARS cases in the literature are for prompt exposures (duration less than 1 min) for nuclear accident victims. A typical SPE imposes a protracted exposure rather than a prompt one. Prompt radiation exposure is generally more effective in causing ARS than a protracted exposure with the same cumulative dose, due to the possibility of biological repair and recovery of bodily systems during a protracted exposure (NCRP 2000; Anno et al. 1996). A realistic evaluation of possible ARS induced by serious SPEs must incorporate the sparing effects of biological repair and recovery.

The possible acute health effects to interplanetary crews from large SPEs have previously been analyzed by some researchers. To our knowledge, the first evaluation was done with a lethal-potentially lethal model (Curtis 1986). Another response model developed by the U.S. military for nuclear warfare (Jones 1981) was used to investigate the blood-forming organ (BFO) effects for the exposure during an August 1972 event (Wilson et al. 1997a). In response to the recently enhanced interest on early radiation effects due to a program of lunar missions by the National Aeronautics and Space Administration (NASA) within the next decade, we present in this report a novel modeling approach to examine the possible early effects on crews from exposure to some historically large SPEs in space missions beyond LEO. A collection of models, implemented in the Radiation-Induced Performance Decrement (RIPD) code, describe the dose- and time-dependent early human responses to various types of ionizing radiation. Based on sound radiobiological principles, these models can be easily adapted to incorporate particle- and energy-specific RBEs, and different exposure histories including multiple prompt and/or protracted events (Anno et al. 1996).

AQ: A

MATERIALS AND METHODS

Approach to space radiation evaluation

To predict the propagation and interaction properties of the energetic nucleons of an SPE through various media, the Baryon radiation transport (BRYNTRN) code (Cucinotta et al. 1994a) was used. This code includes the transport of high-energy light ions with atomic number $Z \leq 2$ (n, p, d, t, h, and α) and solves the fundamental Boltzmann transport equation. With the straight ahead approximation, the transport equation is written as (Wilson et al. 1991):

$$\left[\frac{\partial}{\partial x} - \frac{\partial}{\partial E}\tilde{S}_j(E) + \sigma_j(E)\right]\phi_j(x, E) = \sum_{k \geq j}\int_E^\infty \sigma_{jk}(E, E')\phi_k(x, E')dE', \quad (1)$$

where

$\phi_j(x,E)$ = flux of ions of type j with atomic mass A_j having energy E (in units of MeV amu^{-1}) at spatial location x;
σ_j = macroscopic total nuclear-absorption cross sections;
$\tilde{S}_j$ = change in E per unit distance; and
σ_{jk} = differential nuclear-interaction cross sections.

To evaluate the flux of particles of type j with energy E, the input database required consists of the stopping power, the macroscopic total nuclear cross sections, and the differential nuclear-interaction cross sections. The differential cross sections σ_{jk} describe the production of type j particles with energy E by type k particles of energies $E' > E$. These data are those compiled for the present BRYNTRN code (Cucinotta et al. 1994; Wilson et al. 1995).

Table 1. Particle RBE (NCRP 2000) and the RBE for neutrons suggested by Wilson *et al.* (2002) for deterministic effects.

Particle type	RBE value	
	NCRP	Suggested by Wilson *et al.*
Less than 1 MeV neutrons	RBE (fission neutrons)	5.0
1 to 5 MeV neutrons	6.0	
5 to 50 MeV neutrons	3.5	
Above 25 MeV neutrons	RBE (not more than those of 1–25 MeV neutrons)	3.5
Protons >2 MeV	1.5	
Heavy ions (helium, carbon, neon, argon)	2.5	
Heavy ions, all others	2.5	

The absorbed dose D due to energy deposition at given location x by all particles is calculated according to

$$D(x) = \sum_j \int_0^\infty S_j(E)\phi_j(x,E)dE. \quad (2)$$

Organ dose assessment at a specific anatomical location is calculated with the point particle fluxes for given number of rays that traverse various media, such as spacecraft, equipment, the tissue equivalent material, and any other media on the path of the ray. Each separate medium's thickness distribution along a ray surrounding a specific organ at a specific position inside spacecraft can be generated using the NASA-developed ray tracing model based on the CAD tool of ProE (Ponomarev et al. 2007), which uses an evenly spaced distribution of the given number of rays over a 4π solid angle. In the current study, a typical shield configuration was approximated as a spherical structure for a spacesuit during Extra Vehicular Activity (EVA) and for the equipment room of a spacecraft. For an astronaut organ dose assessment, the human body geometry is based on the 50th percentile United States Air Force male in the standing position used by the Computerized Anatomical Man (CAM) model (Billings and Yucker 1973).

For the deterministic late effects, recently the National Council for Radiological Protection (NCRP 2000) has recommended that dose rate limitations be made on gray-equivalent (Gy-eq) rates (i.e., the organ dose in *gray* multiplied by the relevant RBE for the specific organ and radiation). We do not expect RBE values for early effects to differ substantially from late effects for protons and use these values for acute effect predictions in the present model. For the estimation of acute effects from an intense solar particle event on lunar or Mars missions during transition and on surface, this new dosimetric quantity of Gy-eq (G_T) was implemented using the NCRP's RBE and the suggested definition of neutron RBE (Wilson et al. 2002) for a full definition of neutron RBE:

$$G_T = RBE_j \times D_T, \quad (3)$$

where RBE_j is a recommended value for relative biological effectiveness for deterministic effects for a given particle type j, and D_T is the mean absorbed dose in an organ or tissue. Table 1 shows the RBE as given by NCRP and the suggested RBE values for neutron fields. T1

Table 2 shows estimates of various dosimetric quantities from 3 historically large events (August 1972 SPE, October 1989 SPE, and September 1989 SPE) for their total event spectra and their maximal hourly rates at the peak time inside a typical equipment room of a spacecraft (an aluminum sphere of 5 g cm^{-2} thickness) and spacesuit during EVA (an aluminum sphere of 0.3 g cm^{-2} thickness) in interplanetary space. The detailed hourly rates have been accounted to find the maximal hourly dosimetric quantities for August 1972 SPE, while one tenth of total spectra of October and September 1989 T2

Table 2. Dosimetry quantities in interplanetary space from total event spectra and maximal hourly rates of three large SPEs.

Dosimetry quantities	August 1972 SPE		October 1989 SPE		September 1989 SPE	
	EVA	Spacecraft	EVA	Spacecraft	EVA	Spacecraft
Total spectrum						
D_{skin}, cGy	3215.00	269.50	2599.00	145.40	768.20	53.42
$G_{stomach}$, cGy-Eq	41.64	16.96	43.36	24.94	18.58	11.23
G_{BFO}, cGy-Eq	138.40	46.25	95.52	45.41	37.87	19.29
E, cSv	302.40	61.25	200.20	49.00	68.65	20.15
$\dot{D}_{skin}$, cGy h^{-1}	980.90	28.37	259.90	14.54	76.82	5.34
Maximal hourly rate						
$\dot{G}_{stomach}$, cGy-Eq h^{-1}	12.00	7.74	4.36	2.49	1.86	1.12
$\dot{G}_{BFO}$, cGy-Eq h^{-1}	22.21	12.34	9.55	4.54	3.79	1.93
$\dot{E}$, cSv h^{-1}	46.73	12.44	20.02	4.90	6.87	2.02

Table 3. The variation of stomach doses at 10 specific sites.

	Stomach site #	August 1972 SPE	
		EVA	Spacecraft
Total spectrum, $G_{stomach}$, cGy-eq	1	17.42	7.80
	2	110.07	35.97
	3	30.71	12.66
	4	20.05	8.87
	5	115.51	37.12
	6	28.58	11.77
	7	84.07	29.29
	8	122.67	39.40
	9	21.86	9.52
	10	92.68	30.29
	Mean $\pm$ σ	64.36 $\pm$ 44.32	22.27 $\pm$ 13.21
Maximal hourly rate $\dot{G}_{stomach}$, cGy-eq h^{-1}	1	7.67	5.25
	2	17.99	10.06
	3	9.65	6.32
	4	8.24	5.59
	5	17.92	9.85
	6	9.20	6.05
	7	15.66	9.14
	8	18.62	10.16
	9	8.45	5.70
	10	15.71	8.91
	Mean $\pm$ σ	12.91 $\pm$ 4.63	7.7 $\pm$ 2.08

SPEs was taken, respectively, as the hourly rate at the peak period, which should be a conservative estimate.

To find the variation of prodromal risk related to dose variation across the stomach, 10 specific stomach sites were investigated for the human body geometry using the CAM model (Atwell 1994). The considerable variance of doses within the stomach in Table 3 is caused by the characteristic spectra of particle fluence at each site, which is modified significantly by body-shielding effects at each site.

RIPD models

RIPD radiobiological models represent over a decade of endeavors by a group of research scientists in the Intermediate Dose and Human Response Programs sponsored by the Defense Nuclear Agency in the 1980's and 1990's (Anno et al. 1996), with a mission to provide a symptomatology basis for assessing early functional impairment of individuals who may be involved in civil defense and various military activities in the event of a nuclear attack. These models utilized six sign/symptom (S/S) categories of ARS: upper gastrointestinal distress (UG), fatigability and weakness (FW), lower gastrointestinal distress (LG), hypotension (HY), infection and bleeding (IB), and fluid loss and electrolyte imbalance (FL). In initial work (Anno et al. 1985), the severity of each of these S/S categories was described empirically as a function of absorbed dose and time-after-exposure for prompt exposures. In later work, physiologically based models were developed (Anno et al. 1991, 1996) and incorporated into the RIPD code (Matheson et al. 1995) to estimate the S/S severities for protracted exposures. The models in RIPD have inter-correlation as shown in Fig. 1. They include four stand-alone models (lethality, prodromal UG, LG, and FW), which require only the exposure dose and/or dose rate as input, and five dependent models (ovals in Fig. 1), with input from the output of the stand-alone models.

The lethality model (Jones et al. 1994) in RIPD gives the incidence of mortality by calculating the cell kinetics of myelopoiesis under irradiation, either prompt or protracted. The model calculates an equivalent prompt dose (EPD). For a given protracted exposure sequence, the EPD is the single prompt dose that produces the same

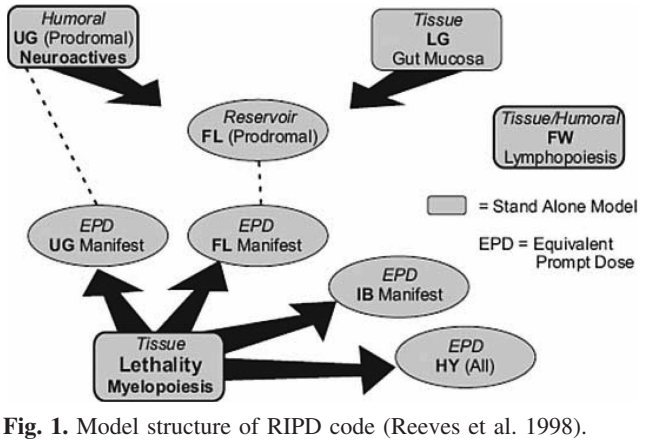

Fig. 1. Model structure of RIPD code (Reeves et al. 1998).

Table 4. Textual descriptions of the symptom severity level and acute radiation sickness.

Severity level	UG	LG	FW	HY	IB	FL
1	No effect	No effect	No effect	No effect	No effect	No effect
2	Upset stomach, clammy and sweaty, mouth waters	Feels uncomfortable urge to have bowel movement	Somewhat tired, with mild weakness	Slightly light-headed	Mild fever and headache	Thirsty and has dry mouth, weak and faint
3	Nauseated, considerable sweating, swallows frequently to avoid vomiting	Occasional diarrhea	Tired, with moderate weakness	Unsteady upon standing quickly	Joints ache, considerable sweating, moderate fever, no appetite, sores in mouth and throat	Very dry mouth and throat, headache, rapid heartbeat
4	Vomited once or twice, nauseated, and may vomit again	Frequent diarrhea and cramps	Very tired and weak	Faints upon standing quickly	Shakes, chills, and aches all over, difficulty in stopping any bleeding	Extremely dry mouth, throat, and skin, very painful headache, difficulty moving, short of breath, burning skin and eyes
5	Vomited several times, including the dry heaves, severely nauseated, and will soon vomit again	Uncontrollable diarrhea and painful cramps	Exhausted, with almost no strength	In shock, breathing rapidly and shallowly, motionless, skin cold, clammy and very pale	Delirious, overwhelming infections, can not stop any bleeding	Prostrate

marrow cell population nadir in the myelopoiesis lethality model as the protracted sequence. The probability of mortality is calculated with the EPD and a lognormal dose-response function (Anno et al. 2003). The estimation of severity of UG, FL, IB, and HY with the dependent models is also based on the calculated EPD.

The other three stand-alone models were developed and implemented by Anno et al. (1991, 1996), also taking into account the sparing effect of protracted exposure. The UG model calculates the kinetics of the production and metabolic clearing of toxins within bodily fluids, the LG model calculates the cellular kinetics of intestinal mucosa, and the FW model calculates the kinetics of lymphocytes and the resulting cytokine production. Each model employs a set of differential (rate) equations emulating relevant biological processes and containing the radiation dose and/or dose rate as a driving term causing damage and/or illness. For each model, a variable such as a toxin level or a cellular population level determines the severity of symptoms. The model equations and parameters arise from basic research in radiobiology and radiation oncology with all models adjusted to the best available human data.

The correlation of incidence as well as severity of various symptoms with exposed dose and dose rate was conducted by performing maximum likelihood probit analysis of empirical data (Anno et al. 1985). While severity is a measure of the effect on a particular individual, incidence is a population-based measure of the effect on a certain group, i.e., at some specified dose level, incidence quantifies the proportion of individuals expected to respond according to a defined level of severity. The main body of empirical data includes effects on victims of nuclear radiation accidents and clinical accounts of cancer patients who received Total Body Irradiation (TBI) therapy from the 1940's to the 1980's. Each S/S category described above was scaled from 1 to 5 with descriptive levels of increasing severity, based on the medical records and common clinical practice, with Level 1 being normal and Level 5 exhibiting the most severe state of the syndrome (Table 4) (Matheson et al. 1996). Then a temporal response pattern for each syndrome was estimated for various ranges of prompt radiation exposure, including the onset, duration, and time-dependent severity. The protracted irradiation cases were treated similarly to the EPD approach, with consideration of sparing effects due to biological recovery that modify the level of response.

Each of the kinetic models is based on sound radiobiological principles and is consistent with the substantial available empirical data. Some animal models (dogs, cats, monkeys, and ferrets) were also used to unveil mechanisms and pathways of the syndromes induced from ionizing radiation damage (Anno et al. 1996), based on the findings that ARS in human and different mammal species are broadly similar (Guskova et al. 2001).

Fig. 2 shows a sample calculation with the RIPD UG model demonstrating the sparing effect of protracted

balt5/zhl-hp/zhl-hp/zhl00409/zhl5181-09z | xppws | S=1 | 2/2/09 | 12:12 | Art: 191045 | Input-8000

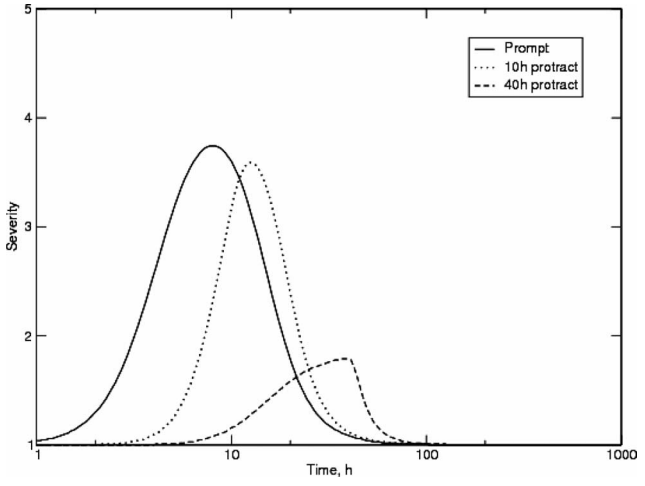

Fig. 2. Sparing UG effect of protracted radiation of a 200 cGy free-in-air gamma ray.

exposure. A 200 cGy free-in-air (FIA) prompt gamma-ray exposure will cause a 3.7 peak severity level of UG distress for a typical individual. For the same dose delivered at a constant dose rate over 10 h, the peak severity of UG effect decreases to 3.6 with a later onset. If the same dose is delivered at a constant dose rate over 40 h, the peak severity is 1.8. Clearly, protraction of the dose over 2 d causes substantial reduction in the predicted severity of illness; however, the fractional severity levels should be interpreted with caution. Strictly speaking, the UG severity scale is an ordinal scale defined only at integer values as shown in Table 4. In an average sense (over a large population), the actual severity of illness, by whatever measure, will increase monotonically with dose in a continuous fashion as does the RIPD-calculated UG severity. However, confounding variables for a given individual will cause the actual severity of illness at a fixed dose and duration of exposure to vary from individual to individual. Certainly, differences in severity level of a few tenths should not be considered significant when predicting the response of one or a few individuals.

The RIPD code can also estimate the performance degradation for various military tasks due to ARS. Performance is calculated according to the logistic function:

$$P = \left[1.0 + EXP\left(- \sum_{i=1-6} \beta_i X_i + C \right) \right]^{-1}, \qquad (4)$$

where

X_i = the severity of the six syndromes;
β_i = the weight of regression coefficients for a task; and
C = a constant term from regression analysis.

Though the performance calculation in RIPD code is defined to evaluate combat effectiveness in a military context (Anno et al. 1984), it can be used in any radiation environment for consequence assessment and planning.

The RIPD code also considers human response for neutron and mixed gamma/neutron exposure, with user-defined RBEs for different endpoints. Extension to accommodate other radiation appropriate for space radiation risk assessment may be done with the RBEs described earlier. Another helpful feature is that the exposure period can be as long as 1 wk, with any complex dose rate history. Also, human response in terms of severity of illness and performance capability, as well as incidence of the UG and FW syndromes and mortality, can be calculated up to 1,000 h (about 6 wk) after start of exposure (Anno et al. 1996).

RESULTS AND DISCUSSION

In this section we present the results of RIPD modeling to investigate the acute effects of the largest SPEs ever recorded based on their temporal dose-rate profile.

As described above, the RIPD models were built upon empirical data obtained from exposures to gamma-ray irradiation. Organ dose calculations using the BRYNTRN and CAM models were expressed in terms of the dosimetric quantity Gy-eq (G_T), determined using the NCRP's RBE values and the suggested definition of neutron RBEs (Wilson et al. 2002) as shown in Table 1. However, there is a subtle issue on converting the FIA dose (or dose rate) to midline tissue (MLT) dose (or dose rate), which is the driving term to cause the neuroactive agents' modulation of the bodily system. The RIPD models used a simple linear conversion FIA = 1.5 · MLT for dose or dose rate. As the gamma rays attenuate almost linearly with the depth of media, this treatment is quite reasonable. But for protons, due to the well-known Bragg-peak profile, the same relationship between FIA dose and MLT dose is not applicable. Using the skin dosage obtained from the transport calculation will greatly overestimate the prodromal effects since the body dermal tissue more effectively shields protons than it does gamma rays. Fig. 3a shows that, within a spacesuit outside a spacecraft, the skin dose rate at the peak of the August 1972 event can be several hundredfold times that for the BFOs. With the shielding of a typical spacecraft (5 g cm^{-2}), the ratio of skin to BFO dose rate at the peak decreases to about 2 (Fig. 3b). To be consistent with the procedure of the RIPD code, in the following calculations we scale the BFO dose-equivalent calculated by BRYNTRN and CAM with a factor 1/1.065 = 0.9 to estimate an MLT dose rate, which the RIPD code uses

balt5/zhl-hp/zhl-hp/zhl00409/zhl5181-09z | xppws | S=1 | 2/2/09 | 12:12 | Art: 191045 | Input-8000

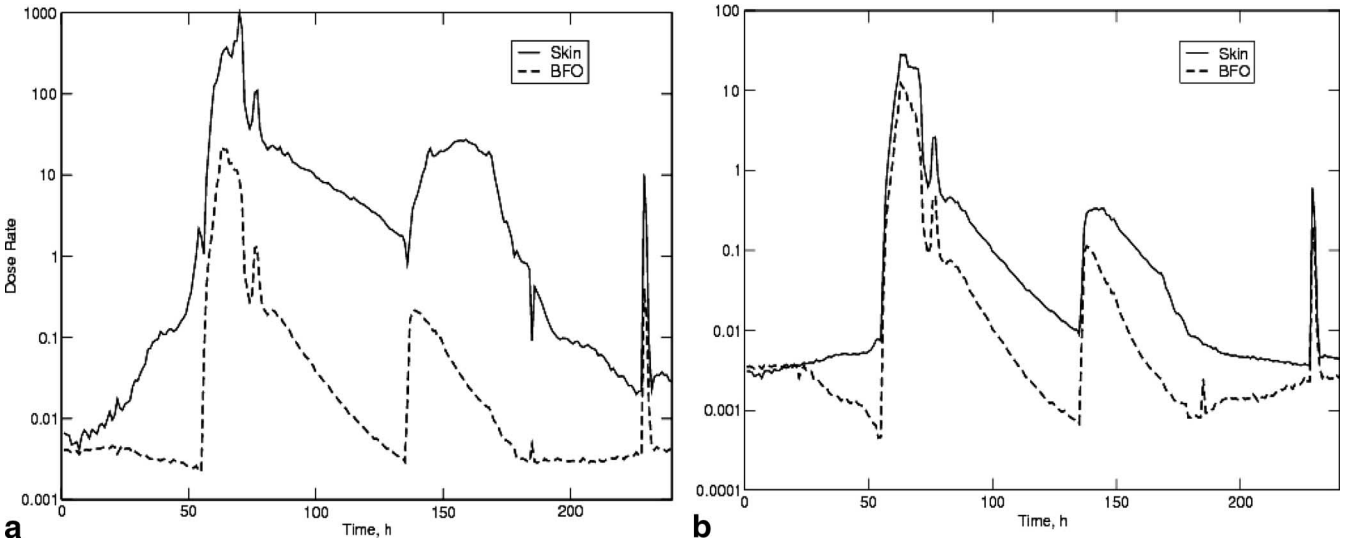

Fig. 3. The skin and BFO dose rates within a spacesuit (0.3 g cm^{-2}) (a) and inside a spacecraft (5.0 g cm^{-2}) (b). The unit for skin dose rate is cGy h^{-1} while for BFO is cGy-eq h^{-1}.

for gamma-ray prodromal effects. To obtain FIA dose rates as needed for RIPD input, we scale the MLT dose rate with a factor 1.5.

ARS effects for crews inside spacecraft during August 1972 SPE peak

The inside-spacecraft modeling starts when the calculated FIA dose rate exceeds 0.1 cGy-eq h^{-1}, which is required by the RIPD software as a threshold to cause human acute effects. From the calculation of the August 1972 SPE, a male crewmember behind a typical spacecraft shielding (5.0 g cm^{-2}) would have 24-h consecutive exposure above this limit (Fig. 3b). After that period, there are several other points in the dose-rate profile that are slightly larger than 0.1 cGy-eq h^{-1}. For simplicity, we did not consider them. The peak BFO dose rate appeared at the 7th hour from the onset of organ-sensible flux, with a value of 12.34 cGy-eq h^{-1} (Fig. 3b). The UG response has a maximum value of 2.0 at the 16th hour, and returns to normal after the end of this period (Fig. 4). The UG syndrome is quite mild and with a low expected incidence of 2% (with 95% confidence limits of 0 to 35%). According to the RIPD documentation, only sensitive personnel would manifest some upset in stomach, feeling clammy and sweaty, with mouth watering and swallowing frequently. No vomiting would occur. A peak in FW severity of about 1.6 appears within a few hours after that of UG, but persists and rises to a level of about 1.8 at 1,000 h. Both levels of severity indicate a rather mild fatigability and weakness. The expected incidence of FW is 17% (with 95% confidence bounds of 3 to 34%). The low incidence and severity of acute effects indicate that the typical spacecraft shielding (5.0 g cm^{-2}) is good enough to attenuate the SPE of the historical worst case to avoid acute injury to male crews. However, the persistence of the mild FW syndrome for such a long time period should be of concern for the health of astronauts in the high risk environment in space.

A doubly intense event

Calculations have been carried out for even worse cases than August 1972 event. Although the August 1972 event is the largest event for which detailed observations are available, there is still some uncertainty in the size of events that astronauts may encounter. Nitrates from ice-core samples that have been analyzed by McCraken et al. (2001) suggest a small number of events of larger size since the 15th century; however, detailed information

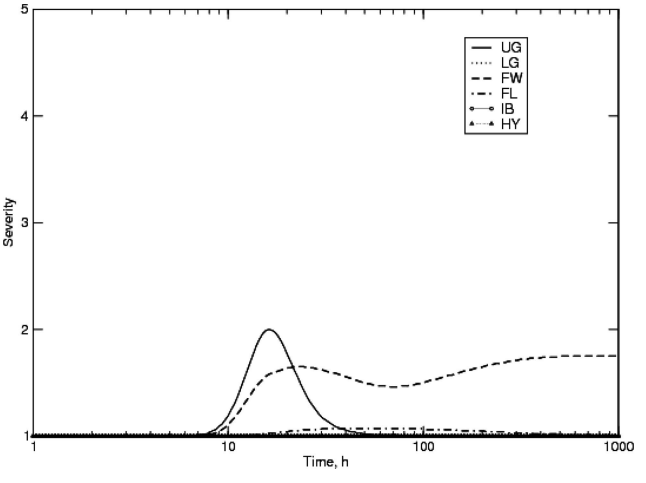

Fig. 4. Acute response of male astronauts inside a spacecraft (5.0 g cm^{-2}) after the August 1972 event.

balt5/zhl-hp/zhl-hp/zhl00409/zhl5181-09z | xppws | S=1 | 2/2/09 | 12:12 | Art: 191045 | Input-8000

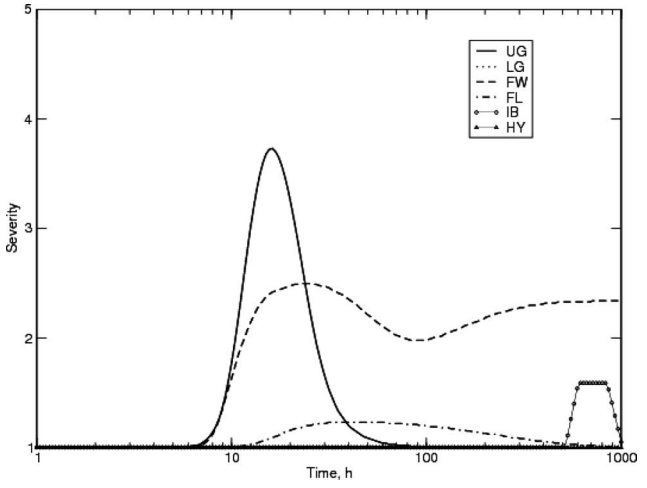

Fig. 5. Acute response of male astronauts inside a spacecraft after a double intensity event of the August 1972 SPE.

on energy spectra and time profiles are not known for these events. The flux spectra of the August 1972 event might be more dangerous than previously thought because the satellite data may have exhibited some saturation and the spectral shape above 60 MeV was not measured (Wilson et al. 1997c). Fig. 5 shows the effects for an SPE with double the intensity of the August 1972 event. The incidences of UG and FW syndromes would be 37 (12 to 69) % and 53 (31 to 74) %, respectively, under this condition. The respective maximum severity would also be raised to 3.7 and 2.5, and the temporal patterns are similar to the previous calculation. The FW effect lasts to the end of this calculation, with a slight improvement at about 100 h. The FL effect is still negligible, with a peak value of 1.2. However, at about 600 h (25 d) there would be a noticeable IB effect (severity 1.6), lasting about 300 h (12.5 d) (Fig. 5). This effect is the manifest illness phase of ARS caused by damage to the BFOs. At higher doses, it is more severe and associated with increasing chance of mortality. According to the RIPD documentation, the male astronauts for the doubly intense event would possibly experience considerable nausea and some vomiting in the prodromal phase, moderate weakness and fatigability for several weeks, and some fever and headache during the manifest phase. No LG and HY effects would be observed at this adverse condition. This calculation indicates that, for an event having double the intensity of the August 1972 SPE, the typical thickness (5.0 g cm^{-2}) of a spacecraft does not provide enough shielding against ARS effects.

Effects of a 3-h EVA during the peak of August 1972 event

Avoidance of vomiting is a high priority for an astronaut in a space suit. If an astronaut inadvertently leaves the shielding of the spacecraft for three hours at the peak of the August 1972 event, the additional exposure would draw him to the threshold of vomiting, though other effects remain mild. Fig. 6a shows that the acute response to exposure with this 3-h EVA plus the remaining time inside the spacecraft is a UG peak severity of about 2.8 and an FW peak and persistent severity of about 2.0.

The additional exposure increases the equivalent prompt dose for lethality from 90 cGy for a crew inside

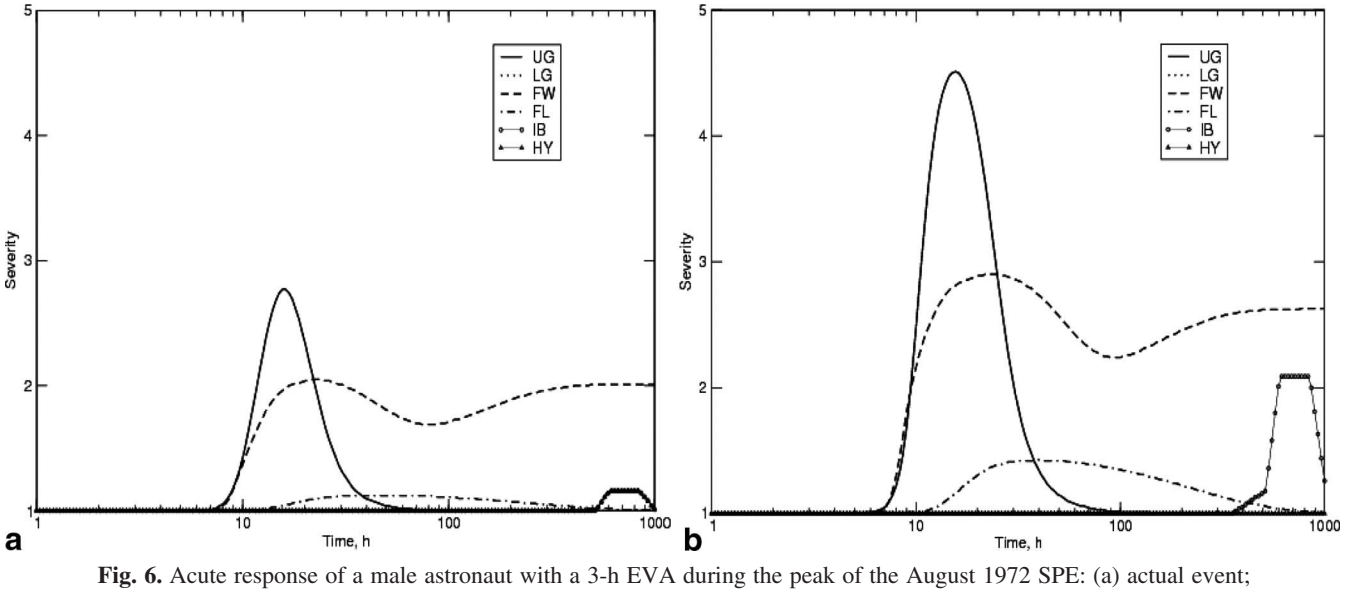

Fig. 6. Acute response of a male astronaut with a 3-h EVA during the peak of the August 1972 SPE: (a) actual event; (b) a doubled intensity event.

a 5.0-g cm^{-2}-thick aluminum spacecraft to 123 cGy including the EVA, but the expected probability of mortality is still less than 0.1% (Anno et al. 2003).

AQ: E Fig. 6a shows that a 3-h EVA during the peak of an event having double the intensity of the August 1972 SPE would certainly induce serious UG distress and a more pronounced FW effect. The peak severities for UG and FW are 4.5 and 2.9, respectively, and the predicted incidence is 71% for both, with a 95% confidence interval of 47–88% for UG and 51–86% for FW. In addition, early FL severity and late IB severity would be 1.4 and 2.1, respectively. Moreover, the additional exposure increases the equivalent prompt dose for lethality from 169 cGy for a crew always inside the spacecraft to 229 cGy including the EVA, raising the probability of mortality from 0.3% to 3.6%. These estimates show that a 3-h EVA during a double intensity event presents very high risk situation.

UG effect of stomach dose calculation

The above calculations use the MLT dose scaled from the calculated BFO dose. More accurate estimation of human response can be achieved if specific organ doses are used, as recent advances in computational algorithms allow us to do (see Methods and Materials). Our first attempt at such an approach is to refine the UG distress calculation by using the calculated stomach dose rate for the August 1972 event. The UG model in the RIPD code considers the dynamics of radio-induced toxin released from specific cells (e.g., enterochromaffin cells, enteroendocrine cells, etc.) in the gut (Anno et al. 1996). These target cells are subject to different exposures due to their different locations, and may cause variance in the calculation of the severity of syndromes.

F7 Fig. 7 shows that the UG distress calculated with average stomach dose rates is significantly milder than that calculated from MLT dose rates. Using the maximum dose rates among the calculated 10 specific sites of the stomach (Table 3), the peak severity of UG increased from 1.4 for the average dose rate to 1.8, still less than the 2.0 calculated from the scaled BFO dose rates. Variation of dose rates for specific sites of the CAM organs (e.g., the stomach) seems to offer an attractive way to estimate uncertainty of acute effects risk using the RIPD models. However, the details of organ dose rates were not considered at the time the RIPD models were developed. We will need to reevaluate the dynamical system (i.e., equations, parameters, etc.) of different endpoints in order to switch from whole-body exposure to specific organ dose rates.

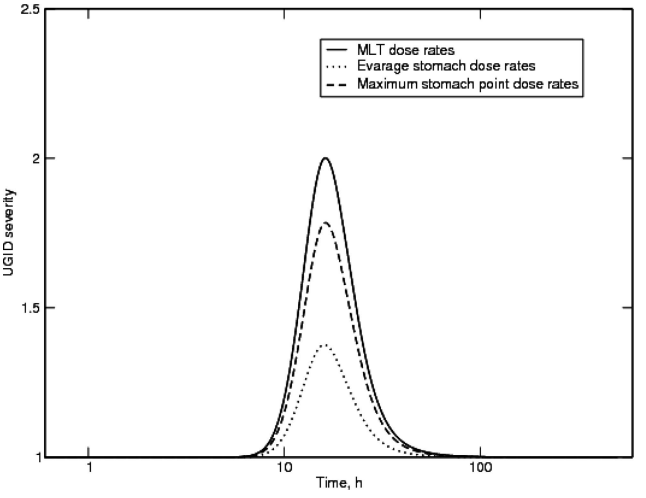

Fig. 7. Calculated UG distress of CAM inside spacecraft after a 30-h exposure during the peak of the August 1972 event, from different dose rates.

Performance degradation after the August 1972 event

Besides the severity of the various manifestations of radiation sickness, the RIPD code can also calculate altered performance due to radiation injury (Anno et al. 1996). Though the performance degradation algorithm was developed to evaluate the residual performance capability of a combat soldier, such calculations should be of great value for operational management of space exploration in case of a large scale radiation event. The RIPD code includes quantitative estimates of performance vs. dose and time-after-exposure for members of an artillery crew, a fire direction center, a tank crew, an antitank crew, and dismounted infantry. Among these various military tasks, the tank commander may be most suited for estimating the operational effectiveness of an astronaut, since both are inside vessels with limited operating space and their tasks are generally not physically demanding as are those of an artillery or tank crew loader.

F8 Fig. 8 shows performance capability predicted by the RIPD code for the tasks of a tank commander after exposure by the August 1972 SPE and a double intensity event, both inside a typical spacecraft (5.0 g cm^{-2}). The calculation shows a nadir in performance during the peak of the August 1972 event, with a value of 0.78, indicating that typical tasks would take (1/0.78) = 1.28 times as long as normal for completion. In a military context, performance better than 0.75 is considered as operationally effective (Anno et al. 1996). The nadir of performance is coincident with the peak of UG distress (Fig. 4), as the UG distress syndrome is among the most important factors compromising performance (Anno et al. 1996). However, performance degradation persists until

balt5/zhl-hp/zhl-hp/zhl00409/zhl5181-09z | xppws | S=1 | 2/2/09 | 12:12 | Art: 191045 | Input-8000

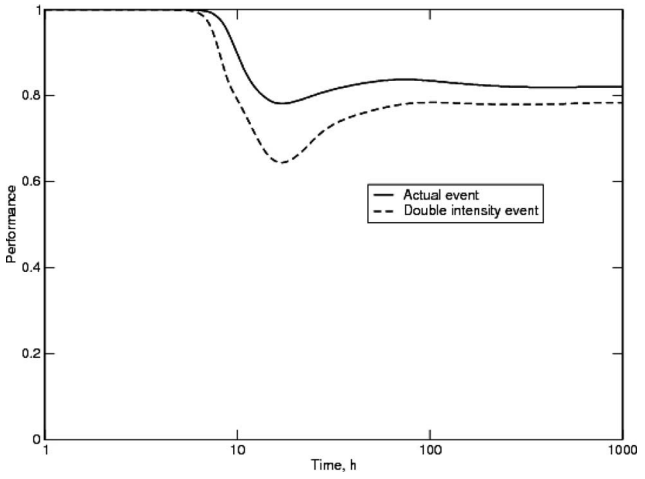

Fig. 8. Performance reduction of astronauts inside a typical spacecraft after the August 1972 event and a double intensity event.

the end of the calculation, indicating that FW effects (Fig. 4) are similarly important. Such persistent degradation is certainly an operational concern for astronauts, though the scale of the calculated performance is in the range of operationally effective (around 0.82 after the prodromal phase).

For the double intensity event, Fig. 8 shows that crews inside a typical spacecraft would experience a significant period of time with reduced operational capability (about 38 h below 0.75). How to manage the key personnel of an operation to get through this critical period should be an important issue for an interplanetary trip.

Effects of multiple SPEs

Historically, multiple SPEs with hazardous flux have occurred within a very short period of time. The pair of events in 1989 listed in Table 2 is such an example. For an interplanetary mission lasting several months or more, it is possible that a crew could be exposed to a series of such events. We used the RIPD code to simulate the possible adverse effects for such events. The results in Table 5 show how the interval between a pair of SPEs influences the manifestation of selected endpoints. For each of the pair of events we used the dose-rate profile of the August 1972 SPE behind a typical spacecraft (average shielding of 5.0 g cm^{-2} aluminum equivalent). The same responses for a single event and double intensity event are also listed for comparison.

The calculations indicate that, with a recovery interval of a few days, a second SPE greatly increases the incidence of UG and FW symptoms. The incidences of these two syndromes for a dual event are much larger than the doubled incidences of a single event. On the other hand, Table 5 shows that the peak severities of FW for a dual event are comparable to those of a double intensity event. However, a second SPE of this kind has little impact on the peak severity of UG compared to a single event. It is clear that the RIPD models quantify different sparing effects for human UG and FW syndromes. On this time scale, UG distress is basically a dose-rate driven response while FW is mostly dose driven.

Unfortunately, we could not do calculations with even longer intervals like the two events in 1989 due to the 168-h exposure duration limitation of the RIPD code. Further research is necessary to estimate the health response to multiple-dose scenarios over longer times.

CONCLUSION

In summary, through our model calculations, we predict that the historically large SPE in August 1972 could cause moderate ARS to crews within a typical interplanetary spacecraft, if effective shielding and medical countermeasures such as an antiemetic were not provided. UG and FW symptoms are the most likely and make the largest contribution to operational performance degradation. The UG effects are severe during the peak flux with correlated duration, while FW symptoms are

Table 5. Effect of recovery interval for a dual event, each like the August 1972 SPE.

	UG		FW					
Interval (days)	Incidence (%)	Peak severity	Incidence (%)	Peak severity	IB Peak severity	Nadir	Performance time (h)	At 1,000 h
0	8	2.2	50	2.4	1.5	0.78	40.2	0.85
1	6	2.0	47	2.4	1.4	0.79	64.3	0.84
2	6	2.0	51	2.4	1.4	0.74	88.4	0.78
3	6	2.0	52	2.5	1.3	0.73	112.4	0.77
4	6	2.0	52	2.6	1.3	0.72	136.5	0.77
5	6	2.0	52	2.6	1.2	0.72	160.6	0.76
Single event	2	2.0	17	1.8	1.0	0.78	16.1	0.82
Double intensity event	38	3.7	53	2.5	1.6	0.65	16.1	0.78

persistent and show no sparing effect. For a more intense event, multiple events in a short period of time, or an EVA, severe acute effects that are possibly mission-threatening may occur. It was suggested that, for such cases, more effective shielding like a shelter of approximately 10 g cm^{-2} of aluminum or alternative materials, and some countermeasure tactics such as antibiotics, specific cytokine therapy, etc., are necessary to be provided to the astronaut in deep space (Wilson et al. 1997a). We also show that acute lethality is unlikely for SPEs even two times greater than the 1972 event; however, it is known that a significant increase in risk of cancer death would occur (Cucinotta and Durante 2006).

In this study we used the calculated dosimetric quantity of Gy-eq (G_T) as the equivalent gamma-ray exposure. Though the RBEs for protons and secondary particles suggested (NCRP 2000; Wilson et al. 2002) are reasonable for deterministic effects, it is still uncertain, for different response endpoints, whether the same exposure of space radiation will cause the same effects as the gamma rays. It is desirable to associate each endpoint with a specific RBE, which was considered but not fully validated in the RIPD code for neutrons (Anno et al. 1996). However, endpoint-specific RBEs are generally not available for other particles such as protons.

Other uncertainties in model calculations include the variation in dose distribution in specific organs, dose-rate modifiers, and the role of other space stressors including microgravity. The dose distribution for most SPEs will show larger variation across critical organs than gamma rays. We expect the prediction of organ doses to be very accurate, with errors less than $\pm 10\%$ based on previous work (Cucinotta et al. 2000; Wilson et al. 1997b); however, the possibility of differences in biological response between protons and gamma rays and between animal models and humans needs to be addressed. Also, it is expected that dose-rate effects will be reduced for protons compared to gamma rays because of the high linear energy transfer (LET) component in SPE exposures due to slowing down protons with energies below 5 MeV and nuclear secondaries. The RIPD code used in this study did not consider other stressors such as microgravity that may cause effects synergistic with those of ARS. Because motion sickness is a common event in spaceflight, the impact of space stressors on the risk of vomiting needs to be considered. An accurate consequence assessment and operational planning in space radiation environment of these factors will require further radiobiological data with appropriate animal models to properly address these uncertainties.

Acknowledgements—We wish to extend a note of gratitude to John Moulder for discussions on models of acute risks. Funding for this study was provided by the NASA Space Radiation Program, Risk Assessment Project. One of the authors (GEM) participated with support from the Defense Threat Reduction Agency, Contract DTRA01-03-D-0014-0015.

REFERENCES

Alexander GA, Swartz HM, Amundson SA, Blakely WF, Buddemeier B, Gallez B, Dainiak N, Goans RE, Hayes RB, Lowry PC, Noska MA, Okunieff P, Salner AL, Schauer DA, Trompier F, Turteltaub KW, Voisin P, Wiley AL Jr, Wilkins R. BiodosEPR-2006 meeting: Acute dosimetry consensus committee recommendations on biodosimetry applications in events involving use of radiation by terrorists and radiation accidents. Radiat Measurements 42:972–996; 2007.

Anno GH, Wilson DB, Dore MA. Symptomatology of acute radiation effects in humans after exposure to doses of 75 to 4500 rads (cGy) free-in-air. Alexandria, VA: Defense Nuclear Agency; DNA-TR-85-0; 1984.

Anno GH, Wilson DB, Baum SJ. Severity levels and symptom complexes for acute radiation sickness: description and quantification. Alexandria, VA: Defense Nuclear Agency; DNA-TR-86-94; 1985.

Anno GH, Baum SJ, Withers HR, Young RW. Symptomatology of acute radiation effects in humans after exposure to doses of 0.5–30 Gy. Health Phys 56:821–838; 1989.

Anno GH, McClellan GE, Dore MA, Baum SJ. Biological effects of protracted exposure to ionizing radiation: review, analysis, and model development. Alexandria, VA: Defense Nuclear Agency; DNA-TR-90-157; 1991.

Anno GH, McClellan GE, Dore MA. Protracted radiation-induced performance decrement. Alexandria, VA: Defense Nuclear Agency; DNA-TR-95-117, Vol 1; 1996.

Anno GH, Young RW, Bloom RM, Mercier JR. Dose response relationships for acute ionizing-radiation lethality. Health Phys 84:565–575; 2003.

Atwell W. Anatomical models for space radiation applications: an overview. Adv Space Res 14:415–422; 1994.

Billings MP, Yucker WR. The computerized anatomical man (CAM) model. Hanover, MD: Center for Aerospace Information; NASA CR-134043; 1973.

Cucinotta FA. Issues in risk assessment from solar particle events. Radiat Measurements 30:261–268; 1999.

Cucinotta FA, Durante M. Cancer risk from exposure to galactic cosmic rays: implications for space exploration by human beings. Lancet Oncol 7:431–435; 2006.

Cucinotta FA, Wilson JW, Badavi FF. Extension to the BRYNTRN code to monoenergetic light ion beams. Hanover, MD: Center for Aerospace Information; NASA TP-3472; 1994a.

Cucinotta FA, Wilson JW, Townsend LW, Golightly MJ, Weyland M. Analysis of radiation risk from alpha particle component of solar particle events. Adv Space Res 10:661–670; 1994b.

Cucinotta FA, Wilson JW, Williams JR, Dicello JF. Analysis of Mir-18 results for physical and biological dosimetry: radiation shielding effectiveness in LEO. Radiat Measurements 132:181–191; 2000.

Cucinotta FA, Manuel FK, Jones J, Iszaro G, Murrey J, Djojonegro B, Wear M. Space radiation and cataracts in astronauts. Radiat Res 156:460–466; 2001.

Curtis SB Lethal and potentially lethal lesions induced by radiation—a unified repair model. Radiat Res 106:252-270; 1986.

Guskova AK, Baranov AE, Gusev IA. Acute radiation sickness: underlying principles and assessment. In: Gusev IA, Guskova AK, Mettler FA, eds. Medical management of radiation accidents. Washington, DC: CRC Press; 2001: 33–51.

International Commission on Radiological Protection. 1990 recommendations of the International Commission on Radiological Protection. New York: Elsevier Science; ICRP Publication 60; Annals of the ICRP 21; 1991.

Jones TD. Hematologic syndrome in man modeled from mammalian lethality. Health Phys 41:83–103; 1981.

Jones TD, Morris MD, Young RW. Dose-rate RBE factors for photons: hematopoietic syndrome in humans vs. stromal cell cytopenia. Health Phys 67:495–508; 1994.

Katz R, Cucinotta FA. RBE vs. dose for low doses of high LET radiation. Health Phys 60:717–719; 1991.

Matheson LN, Dore MA, Anno GH, McClellan GE. User's manual: radiation-induced performance decrement (RIPD), version 2.0. Alexandria, VA: Defense Nuclear Agency; DNA-TR-95-91; 1995.

Mazur JE, Mason GM, Klecker B, McGuire RE. The energy spectra of solar flare hydrogen, helium, oxygen and iron: evidence for stochastic acceleration. Astrophys J 401:398–410; 1992.

McCracken KG, Dreschhoff GAM, Zeller EJ, Smart DF, Shea MA. Solar cosmic ray events for the period 1561–1994 1. Identification in polar ice, 1561–1950. J Geophys Res 106:21585–21598; 2001.

National Council on Radiation Protection and Measurements. Exposure of the U.S. population from diagnostic medical radiation. Bethesda, MD: NCRP; Report No. 100; 1989.

National Council on Radiation Protection and Measurements. Radiation protection guidance for activities in low-earth orbit. Bethesda, MD: NCRP; Report 132; 2000.

National Council on Radiation Protection and Measurements. Information needed to make radiation protection recommendations for space missions beyond low-earth orbit. Bethesda MD: NCRP; Report No. 153; 2006.

Ponomarev AL, Nounu HN, Hussein HF, Kim MY, Atwell W, Cucinotta FA. NASA-developed ProE-based tool for the ray-tracing of spacecraft geometry to determine radiation doses and particles fluxes in habitable areas of spacecraft and in the human body. Hanover, MD: Center for Aerospace Information; NASA/TP-2007-214770; 2007.

Reames DV. Energetic particle observations and the abundances of elements in the solar corona. In: Domingo V, ed. Coronal streamers, coronal loops, and coronal and solar wind composition. Proceedings of the First SOHO Workshop. Noordwijk, The Netherlands: European Space Agency; SP-348; 1992: 315–323.

Reeves GI, Jarrett DG, Seed TM, King GL, Blakely WF. Proceedings: Triage of irradiated personnel. Bethesda, MD: Armed Forces Radiobiology Research Institute; Special Publication 98-2, DTIC AD A 342949; 1998.

Shea MA, Smart DF. Recent and historical solar proton events. Radiocarbon 34:255–262; 1992.

Townsend LW, Wilson JW, Shinn JL, Curtis SB. Human exposure to large solar particle events in space. Adv Space Res 12:339–348; 1992.

Wilson JW, Khandelwal GS, Shinn JL, Nealy JE, Townsend LW, Cucinotta FA. Simplified model for solar cosmic ray exposure in manned earth orbital flights. Hanover, MD: Center for Aerospace Information; NASA TM-4182; 1990.

Wilson JW, Townsend LW, Schimmerling W, Khandelwal GS, Khan F, Nealy JE, Cucinotta FA, Simonsen LC, Shinn JL, Norbury JW. Application to space exploration. In: Transport methods and interactions for space radiations. Hanover, MD: Center for Aerospace Information; NASA Reference Publication 1257; 1991: 459–517.

Wilson JW, Kim M, Schimmerling W, Badavi FF, Thibeault SA, Cucinotta FA, Shinn JL, Kiefer R. Issues in space radiation protection. Health Phys 68:50–58; 1995.

Wilson JW, Cucinotta FA, Jones TD, Chang CK. Astronaut protection from solar event of August 4, 1972. Hanover, MD: Center for Aerospace Information; NASA-TP 3643; 1997a.

Wilson JW, Miller J, Konradi A, Cucinotta FA. Shielding strategies for human space exploration. Hanover, MD: Center for Aerospace Information; NASA CP 3360; 1997b.

Wilson JW, Simonsen LC, Shinn JL, Dubey RR, Jordan W, Kim MY. Radiation analysis for the human lunar return mission. Hanover, MD: Center for Aerospace Information; NASA TP 3362; 1997c.

Wilson JW, Kim MY, De Angelis G, Cucinotta FA, Yoshizawa N, Badavi FF. Implementation of Gy-Eq for deterministic effects limitation in shield design. J Radiat Res 43:(Suppl):S103–S106; 2002.

■ ■